Monte Carlo simulation of ferroelectric domain growth

B. L. Li,[1,2] X. P. Liu,[1] F. Fang,[1] J. L. Zhu,[2] and J.-M. Liu[1,3,*]
[1]*Nanjing National Laboratory of Microstructures, Nanjing University, Nanjing 210093, China*
[2]*Department of Physics, Tsinghua University, Beijing 10084, China*
[3]*International Center for Materials Physics, Chinese Academy of Sciences, Shenyang, China*
(Received 1 August 2005; revised manuscript received 14 October 2005; published 13 January 2006)

The kinetics of two-dimensional isothermal domain growth in a quenched ferroelectric system is investigated using Monte Carlo simulation based on a realistic Ginzburg-Landau ferroelectric model with cubic-tetragonal (square-rectangle) phase transitions. The evolution of the domain pattern and domain size with annealing time is simulated, and the stability of trijunctions and tetrajunctions of domain walls is analyzed. It is found that in this much realistic model with strong dipole alignment anisotropy and long-range Coulomb interaction, the powerlaw for normal domain growth still stands applicable. Towards the late stage of domain growth, both the average domain area and reciprocal density of domain wall junctions increase linearly with time, and the one-parameter dynamic scaling of the domain growth is demonstrated.

DOI: 10.1103/PhysRevB.73.014107 PACS number(s): 77.80.Dj, 81.30.Hd, 61.72.Mm

I. INTRODUCTION

In the past half century, the domain growth or second phase coarsening in different phase transition systems leading to self-organized pattern formation has been an everlasting interesting subject in statistical physics and materials science, to the best of our knowledge.[1–7] The universal feature of these phase transitions is the self-similarity of the evolved microstructures in terms of size distribution as a function of time and other system parameters during annealing of so-called "quenched" systems, which can be expanded to any system with the interrupt shift of control parameters, more than temperature.[5] When a system is quenched from a high-temperature disordered phase to a temperature below the transition point, a symmetry-broken phase (ordered phase) appears by the formation of ordered domains or second phases. Here, we confine our consideration within the cases of ordered domain separated by domain walls, i.e., multidomained microstructure.[2] Driven by the chemical potential difference between neighboring domains of different sizes, the domain growth is activated by the growth of larger domains in compensation with the shrinking of smaller ones. In other words, minimizing the domain wall energy (interfacial energy) results in the domain growth. For the normal domain growth driven by minimizing the isotropic domain wall energy, it has been indicated that the microstructural evolution can be depicted by the growth kinetics of a unique characteristic length $l(t)$, which marks the characteristic size of formed microstructures. There exists an asymptotic regime in which the characteristic length follows a power-law behavior in time $l(t) \sim t^n$, where n is called the growth exponent.[1,3] Such an asymptotic regime represents a scaling state, that argues that the spatial evolution of the domained structure is (in a statistical sense) independent of time when the domain dimensions are rescaled by $l(t)$. Considered to be a universal feature and playing a central role in understanding the ever more complex systems, the scaling behavior has been revealed in quenched systems for a long time by physicists interested in domain growth and pattern formation.[1,2,4,8]

In addition, the evolution of the domain wall junctions during the domain growth is of interest in terms of topological consideration. A junction is defined as the terminal where three or more domain walls are joined. The number of the walls ended at a given junction is defined as the junction degree. We name a junction terminated with three walls the trijunction, that with four walls the tetrajunction, and so on. The stability of these junctions during domain growth is associated with topological patterns of the multidomained microstructure. It has been well established that the tetrajunction is unstable for normal domain growth and it will decompose into two trijunctions, because the mechanical balance can be satisfied against fluctuations at trijunctions instead of tetrajunctions.[8]

Our understanding about the kinetics of normal domain growth can be mainly ascribed to the Monte Carlo simulation based on models with simple parameter and short-range interactions, such as the kinetic Ising model,[9] the Q-state Potts model,[10–12] the time-dependent Ginzburg-Landau model,[13] the large-N model,[14] and their derived models.[15–20] For systems described by nonconserved order parameter such as multidomained microstructures, a growth exponent $n=\frac{1}{2}$ is well established by minimizing the interfacial energy, if one considers the characteristic length $l(t)$ of the domained structure as a function of time t: $l(t) \sim t^n$, as long as the evolution is approaching to the asymptotic later stage. To understand the result, one can refer to the simple but heuristic argument given by Bray that for nonconserved dynamics the domain with radius R will collapse in a time of order R^2. Therefore, crudely speaking, there will be no domain smaller than $t^{1/2}$ after time t, hence the characteristic domain size is $l(t) \sim t^{1/2}$.[1] When the order parameter is conserved, such as second phase precipitation from a multicomponent solid solution and subsequent coarsening, the exponent is $n=\frac{1}{3}$.[1,3] In a general sense, domain growth or coarsening in tremendous self-assembly systems, whether or not the order parameter is conserved, can be described using the power law with a different growth exponent n.

In spite of the generality of the power law for domain evolution as a general phenomenon in phase transitions

investigated so far,[2–6,9–19] continuous interests in investigating systems with complicated interactions and low symmetry are still reserved. Along this line, many system parameters are believed to have an effect on the kinetics of domain growth, such as the component number of order parameter,[1] conservative condition of order parameters,[1,3] structural anisotropy,[21] defects,[22,23] finite temperature,[3,24] long-range elastic interaction,[25,26] as well as complex interactions engaged in interested systems.[27] In this paper, we perform a Monte Carlo simulation on the kinetics of domain growth in a two-dimensional (2D) lattice based on a realistic Ginzburg-Landau ferroelectric (GLFE) model with a cubic-tetragonal phase transition. In this 2D GLFE lattice, the cubic-rectangle ferroelectric transition is viewed as a square-rectangle transition. We deal with a case where a paraelectric lattice is submitted to a temperature T much lower than its ferroelectric Curie point T_c. Then the lattice is thermally annealed at T and we study the kinetics of domain formation and evolution during the annealing of this GLFE lattice.

However, for a GLFE lattice, minimizing the interfacial energy is no longer the unique drive for the domain growth, because additional Landau potential, long-range Coulomb interaction and polarization orientation anisotropy have to be taken into account. For some FE systems, the long-range elastic interaction associated with the FE phase transitions cannot be neglected either.[28] It is basically believed that the long-range elastic interaction hinders essentially the domain growth or grain coarsening and consequently the well-established power law might not be followed to some extent.[25,26] These additional interactions distinguish the GLFE model from the Ising model or Potts model conventionally employed for simulating the normal domain growth. The GLFE lattice also contains the inhomogeneous domain wall energy and therefore represents a more realistic approach to the kinetics of domain growth in real materials. It is interesting that the simulation reveals a normal domain growth behavior for the GLFE lattice, i.e., the domain growth shows an exponent $n \sim \frac{1}{2}$ over a wide temperature range.

II. MODEL AND PROCEDURE OF SIMULATION

A. Model

Our Monte Carlo simulation is performed on a 2D $N \times N$ lattice with periodic boundary conditions applied. On each lattice site i, an electric dipole is imposed with its moment vector $\boldsymbol{P}(r)=[P_x(r),P_y(r)]$, where $P_x(r)$ and $P_y(r)$ are the two components along the x and y axis, respectively. The energy of the GLFE lattice can be expressed as a function of these moment vectors, of which both the orientation and magnitude are allowed to change.[28–30] By doing so, we assume that the thermal flip of dipoles is the unique mechanism over the phase transition range, considering that other possible ones, such as polarization resonance, are not dominant unless the temperature is extremely low.[28] Referring to the tetragonal structure of typical ferroelectric $BaTiO_3$ below its T_c,[28] each moment vector is allowed to take only four different orientations: $[0,\pm 1]$ and $[\pm 1,0]$, while its magnitude can take any value within (0,1). There are several energy terms which will determine the dipole configuration in the lattice and should be taken into account, including the Landau potential, the dipole-dipole Coulomb interaction, and the gradient energy which gives rise to the domain wall inhomogeneity.[28,30]

What should be pointed out here is that the long-range elastic interaction can be very important for some ferroelectric systems such as $BaTiO_3$ employed as a mode for the present study. As investigated earlier[28,31] and addressed by Arlt,[32] the elastic energy contribution can be dominant and results in a stable striplelike twinned domain structure which might lose its capability to grow and coarsen in a normal manner. Therefore, we will not take into account the contribution of the long-range elastic interaction in the present study, because we focus on the kinetics of normal domain growth in a typical GEFE lattice, as compared to simpler Ising or Potts systems. In fact, the slowing effect of domain growth by the elastic interaction has never been sufficiently verified by simulation since the long-time simulation over several orders of magnitude in time t becomes extremely challenging to conventional computational capability.

For a dipole of moment $\boldsymbol{P}$ at site i, the Landau potential can be expressed as

$$\vec{F}_{ld}(P) = A_1(P_x^2+P_y^2) + A_{11}(P_x^4+P_y^4) + A_{12}P_x^2P_y^2 + A_{111}(P_x^6+P_y^6), \tag{1}$$

where subscript i marks the lattice site, and A_1, A_{11}, A_{12}, and A_{111} are the expansion coefficients. The values of these coefficients will determine the feature of the thermodynamic behavior. For normal ferroelectrics, the first order phase transition will take place if $A_1<0$. At a given temperature T, A_1 can be obtained from

$$A_1 = \alpha(T-T_c), \quad \alpha>0, \tag{2}$$

where α is a constant. If $T<T_c$, A_1 will be negative, thus nonzero spontaneous polarization will take place. The domain wall gradient energy (interfacial energy) for a site i and its neighbor j can be written as

$$F_{gr}(P_{i,j}) = \tfrac{1}{2}[G_{11}(P_{x,x}^2+P_{y,y}^2) + G_{12}P_{x,x}P_{y,y} + G_{44}(P_{x,y}+P_{y,x})^2 + G'_{44}(P_{x,y}-P_{y,x})^2], \tag{3}$$

where $P_{i,j}=\partial P_i/\partial x_j$. In general, the domain wall energy is anisotropic. Since parameters G_{11}, G_{12}, G_{44}, and G'_{44} are all positive, $F_{gr}>0$, in general, favors the homogeneous dipole alignment in the lattice.

The dipole-dipole interaction is expressed by the long-range Coulomb interaction between any couples of dipoles. It can be given in the following form:

$$F_{di}(P_i) = \frac{1}{8\pi\epsilon_0\chi}\sum_{\langle j\rangle}\left[\frac{P(r_i)P(r_j)}{|r_i-r_j|^3} - \frac{3[P(r_i)(r_i-r_j)][P(r_j)(r_i-r_j)]}{|r_i-r_j|^5}\right], \tag{4}$$

where ϵ_0 and χ are the vacuum susceptibility and the relative dielectric susceptibility, $\langle j\rangle$ marks a summation over all sites within a region in a circle with a truncate radius R_T(R_T

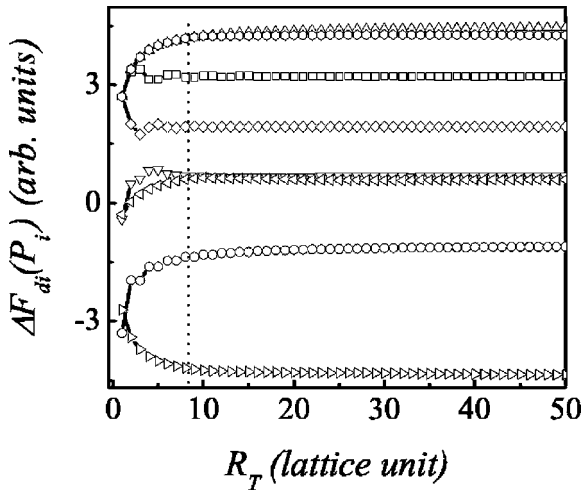

FIG. 1. Calculated difference $\Delta F_{di}(P_i)$ in the dipole-dipole long-range Coulomb interaction before and after an arbitrary dipole flip at site i as a function of truncate radius R_T for eight arbitrarily chosen dipole lattices ($N=500$).

$\rightarrow \infty$) centered at site i, while $P(r_i)$, $P(r_j)$, r_i, and r_j present the moment vectors and the coordinates of sites i and j, respectively.

In a realistic simulation, a finite truncate radius R_T instead of $R_T \rightarrow \infty$ is needed. Nevertheless, the Coulomb interaction is long range and the pair potential does not decrease rapidly with increasing R_T, although each individual term in Eq. (4) decays rapidly with increasing separation $|r_i - r_j|$.[33] Therefore, the Coulomb interaction cannot be truncated at any reasonable distance in a strict sense. A calculation of $F_{di}(P_i)$ by Eq. (4) has to be treated by an Ewald procedure.[34] However, in the present simulation algorithm to be shown below, we only need to evaluate the difference $\Delta F_{di}(P_i)$ associated with a dipole flip at site i from one state to another. We demonstrate numerically that this difference ΔF_{di} as a function of truncate radius R_T changes as $R_T < 8$ and then becomes almost independent of R_T, no matter what the initial lattice configuration is. Figure 1 presents the calculated $\Delta F_{di}(P_i)$ as a function of R_T for randomly chosen 8 lattice configurations, including that with parallel and antiparallel alignments of dipoles. Although the absolute value of $\Delta F_{di}(P_i)$ can be different from case to case, the independence of it on R_T as $R_T \geqslant 8$ is shown for all cases. In fact, we checked with the difference in kinetics of the domain growth at $R_T=8$ and $R_T=20$, and no identifiable difference between them is found. Therefore, in our simulation, a finite cutoff at $R_T=8$ is taken, which is believed to be reliable. Note here that minimizing the Coulomb interaction over the lattice favors a head-to-tail alignment of dipoles.

In sum, the total energy of our system is

$$F_{tl} = \sum_i [F_{ld}(P_i) + F_{gr}(P_i) + F_{di}(P_i)]. \tag{5}$$

The final multidomained microstructure is determined by minimizing the total energy Eq. (5), and, in fact, we see that the different terms favor different dipole alignment configurations. The multidomained microstructure is determined by a compromise among these interactions.

B. Procedure of simulation

Assuming that the thermally activated dipole flip is the unique mechanism in the present GLFE lattice, we perform the simulation via the Metropolis algorithm. First of all, the lattice is initialized in the following way to form a paraelectric system. For each site, two random numbers r_1 and r_2 are generated to decide the orientation and moment of local dipole. Number r_1 is an integer belonging to $[0,1,2,3]$, marking the orientation $[1,0]$, $[0,-1]$, $[-1,0]$, and $[0,1]$, respectively, while r_2 is a real number chosen randomly from interval $(0,1)$. Two interdependent matrices are adopted to restore the orientations and moment magnitudes of all sites. After initialization, we give the system a temperature $T < T_c$ and let the system evolve in isothermal condition. The isothermal annealing is performed in the following procedure. Site i is chosen at random, and then all the energy terms are calculated to obtain F_{tl}. Then a candidate dipole site with new magnitude and orientation is randomly generated. Consequently, F_{tl} is recalculated and compared with the value of F_{tl} before the proposed flip to obtain the difference ΔF of the total energy after and before the proposed flip. The flip is accepted by the probability p_1:

$$p_1 = \begin{cases} \exp(-\Delta F/kT), & \text{if } \Delta F > 0, \\ 1, & \text{if } \Delta F < 0. \end{cases} \tag{6}$$

We generate a random number r_3 within $(0,1)$, and if $r_3 < p_1$ then we accept the proposed flip, otherwise the flip is aborted and the dipole remains unchanged. Then one cycle of the simulation is completed, and another cycle begins until a given number of cycles is completed. The time for simulation is scaled by Monte Carlo step (mcs). One mcs represents $N \times N$ cycles performed. In our simulation, the values of parameters mentioned above are given as follows: $T_c=1.0$, $\alpha=1.0$, $A_{11}=-0.5$, $A_{12}=9.0$, $A_{111}=0.8$, $G_{11}=1.0$, $G_{12}=0.2$, $G_{44}=1.0$, $G'_{44}=1.0$, $R_T=8$, and $N=500$. These parameters refer to a realistic ferroelectric system $BaTiO_3$.[28] It must be pointed out here again that by using the present model one cannot expect to simulate the real domain structure of $BaTiO_3$, where the elastic energy rather than the electric energy (dipole-dipole interaction) is dominant. Here we only investigate the kinetics of the domain growth of a general GLFE model, introducing the long-range coulomb interaction. Thus, the elastic interaction existing in $BaTiO_3$ will be excluded in the present simulation.

III. RESULTS AND DISCUSSION

A. Domain configuration

Figure 2 presents the system energy per site (F_{tl}/N^2) as a function of $\ln(t)$ at four temperatures $T/T_c=0.1$, 0.3, 0.5, and 0.8. The time dependence of F_{tl}/N^2, given a fixed temperature, shows a clear transition regime at an early stage as $t < 400$ mcs, during which the energy declines very rapidly. This regime corresponds to a rapid isothermal ferroelectric

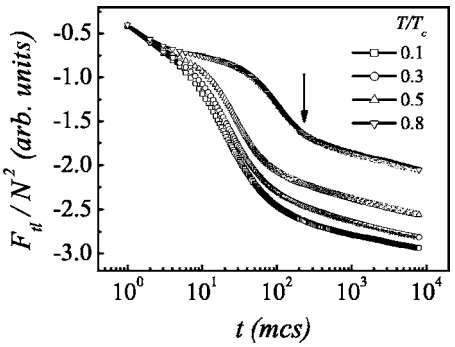

FIG. 2. Total energy per site (F_{tl}/N^2) as a function of $\ln(t)$ at four temperatures $T/T_c=0.1$, 0.3, 0.5, and 0.8, respectively. The arrow indicates the boundary between the earlier state and the late stage at $T/T_c=0.8$.

phase transition of the lattice from the paraelectric state. In this regime, the energy falls more rapidly at a lower T, indicating an earlier completion of the phase transition. Toward the late asymptotic regime, one observes a linear decay of F_{tl}/N^2 with $\ln(t)$, corresponding to the domain growth period which is focused in this paper. The arrow in Fig. 2 indicates the boundary between the two regimes discussed above.

We present as an example the temporal evolution of domain configuration at $T/T_c=0.5$, as shown in Fig. 3. The four patterns are snapshotted at $t=800$, 2800, 4800, and 8000 mcs, respectively. The polarization orientations of domains are distinguished by four different gray levels. The black area stands for $[1,0]$, dark gray for $[0,1]$, light gray for $[0,-1]$, and white for $[-1,0]$, as indicated by the arrows in Fig. 3(d). The profile of magnitude is omitted here because the dipole magnitude within one domain is roughly identical, although the dipoles on domain walls may have smaller magnitude. Keep in mind that the annealing temperature is far below T_c and the polarization is almost saturated after the transient regime ($t\sim 400$ mcs). In Fig. 4 we present the four snapshot images of the domain patterns at $t=8000$ mcs for $T/T_c=0.1$, 0.3, 0.5, and 0.8, respectively. Several interesting features as revealed in Figs. 3 and 4 are worth mentioning. First, significant domain growth phenomenon is revealed, and the kinetics of domain growth is considerably T dependent. Given a fixed t, the domain growth is more rapid at a higher T because of the thermal flip process contributing to the domain growth. Second, the individual domain pattern is not a circle but shows strong anisotropy. Most of the domain walls are straight instead of curved as exhibited in systems of isotropic interfacial energy. Almost half of the domain walls incline at 45° with respect to the x axis or y axis, indicating 90° domain walls, while other walls align vertically or horizontally, representing the 180° walls. The coexistence of both 90° walls and 180° walls is observed. What should be noted here is that we do not take the long-range elastic energy into account in our simulation. Thus, no long-striped domain patterns often observed experimentally are revealed here. Finally, both trijunctions and tetrajunctions are observed, predicting the eminent role of the dipole alignment anisotropy in modulating the domain growth. As reported earlier,[7,8,17] in the domain growth of isotropic interfacial energy, the tetrajunction is unstable against fluctuations and it will decompose into two trijunctions. However, in the present GLFE lattice, quite a number of tetrajunctions can survive for a long time, although the number of tetrajunc-

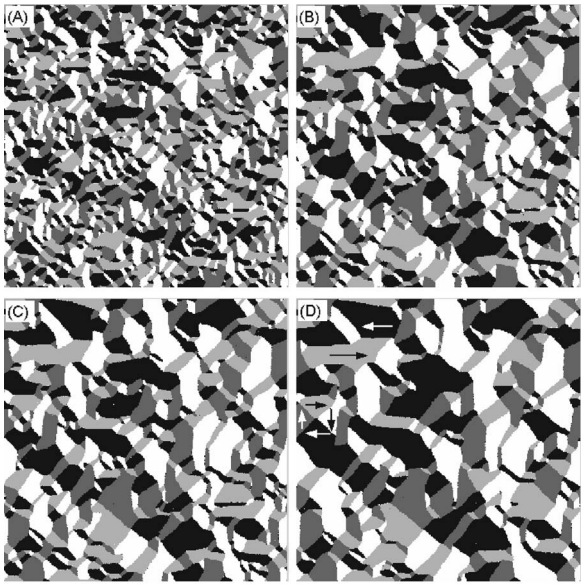

$T/T_c=0.5$

FIG. 3. Temporal evolution of domain patterns at $T/T_c=0.5$. (a) $t=800$ mcs; (b) $t=2800$ mcs; (c) $t=4800$ mcs; (d) $t=8000$ mcs. Four types of domains distinguished by the direction of the polarization vector are shown by the four shadows of gray. The relation between the shadow of gray and the direction of the polarization is given by the arrows in (d).

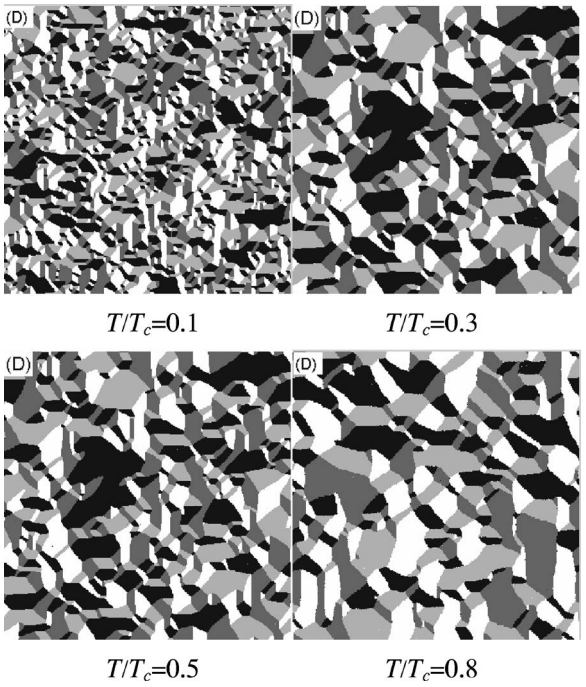

FIG. 4. Snapshot images of domain patterns at $t=8000$ mcs for $T/T_c=0.1$, 0.3, 0.5, and 0.8.

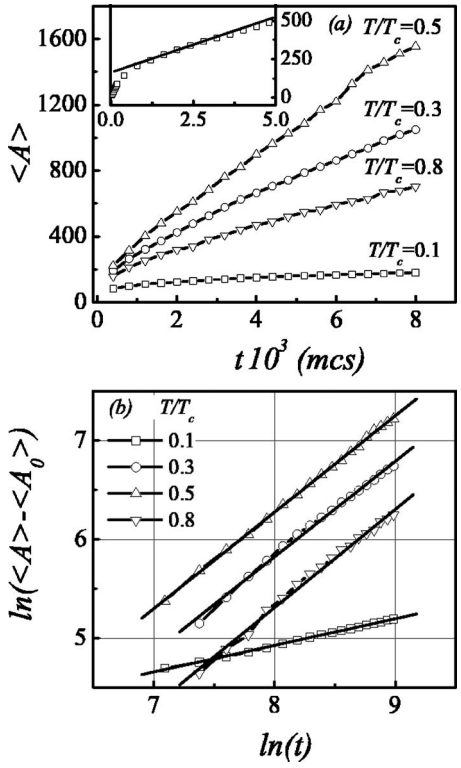

FIG. 5. (a) Average domain area $\langle A\rangle$ as a function of time t, and (b) $\ln(\langle A(t)\rangle - \langle A_0\rangle)$ as a function of $\ln(t)$ at $T/T_c=0.1$, 0.3, 0.5, and 0.8, respectively. The inset in (a) shows the early stage deviation of the data from the line growth law, and the solid lines in (b) represent the linear fitting.

tions is much less than trijunctions. The coexistence of trijunctions and tetrajunctions is demonstrated here.

To understand the coexistence of 90° and/or 180° domain walls and trijunctions and/or tetrajunctions in the GLFE lattice, one may consult the interactions engaged in the system. As predicted above, the long-range Coulomb interaction favors antiparallel dipole alignment, thus favoring the 180° domain wall, while only minimizing the gradient energy (interfacial energy) will prefer 90° domain walls. Unless the Coulomb interaction is much weaker than the gradient energy, which is not true for the GLFE lattice, the coexistence of 180° and/or 90° domain walls becomes favored. Because of the dipole alignment anisotropy, the domain wall orientation must be either 45°-inclined or vertical and/or horizontal with respect to the x or y axis. Thus the coexistence of trijunctions and/or tetrajunctions is inevitable during the kinetic domain growth process, from the point of view of topological preference. It is therefore concluded that the topological pattern of the GLFE lattice distinguishes essentially from the normal domain growth of isotropic interfacial energy.

B. Kinetics of domain growth

We look at the kinetics of domain growth in the GLFE lattice. The average domain area $\langle A\rangle$ as a function of time t at $T/T_c=0.1$, 0.3, 0.5, and 0.8, is plotted in Fig. 5(a), where $\langle A\rangle$ is derived by dividing the lattice area over the number of domains in the lattice. For all cases, the data are obtained by averaging over ten independent simulation runs. Here we omit the data during the transient regime, in which the domain growth could be much faster. For example, one can refer to the inset of Fig. 5(a) where the data from $t=20$ to 8000 mcs at $T/T_c=0.8$ is shown, and a clear transition regime as $t<400$ mcs is revealed.

In a general sense, given a fixed t for annealing, one sees that $\langle A\rangle$ increases with increasing T as $T=0.1T_c$ to $0.5T_c$, which is easy to understand because of the thermally activated dipole flips. However, at $T=0.8T_c$, the simulated $\langle A\rangle$ is even smaller than those at lower T. The reason lies in the fact that as $T=0.8T_c$, a very high temperature not far from T_c, there appear quite a number of small domains which are generated due to the significant thermal fluctuations and have a very short lifetime. These temporally existed small domains make the calculated $\langle A\rangle$ even smaller than those at lower T, while actually the long lifetime domains are larger than those observed at lower T.

For all cases, $\langle A\rangle$ as a function of time t is well fitted utilizing the power-law $\langle A\rangle - \langle A_0\rangle = t^m$ where $m=2n$ is also the growth exponent, and A_0 is the initial average domain area, obtained by the linear fits to the $\langle A\rangle$ vs t data. The simulated data are replotted in Fig. 5(b). A good linear dependence of $\ln(\langle A(t)\rangle - \langle A_0\rangle)$ on $\ln(t)$ is shown. The growth exponent is $m=0.97\pm0.02$ for $T=0.3T_c$, $m=0.98\pm0.02$ for $T=0.5T_c$, and $m=1.00\pm0.02$ for $T=0.8T_c$, respectively. This demonstrates that the domain growth as exhibited in the present GLFE lattice still follows the kinetics of normal domain growth as well confirmed. For the case of $T/T_c=0.1$, where $\langle A_0\rangle$ is taken as zero, the linear fitting of the data produces an exponent $m=0.269\pm0.002$, much smaller than 1.0 as applied to the other three higher temperatures. Looking back at the domain patterns at $T/T_c=0.1$, as shown in Fig. 4, one may argue that the domain growth is still far from the late stage as $t=8000$ mcs because of significantly frozen dipoleflips. Also, at such a low T, the relative significance of the Coulomb interaction in comparison to the gradient energy becomes even more remarkable. Although the kinetics at such low T is worth further investigation, nevertheless, the power-law behavior is well followed, predicting applicability of the normal growth mode.

C. Evolution of trijunctions and/or tetrajunctions

We evaluate the time dependence of the number of junctions (density of junctions) at different T, as shown in Fig. 6. The number of trijunctions is much higher than that of tetrajunctions, predicting higher stability of the trijunction than the tetrajunction. Given a fixed t, the numbers of both types of junctions decrease with increasing T. Given a fixed T, these numbers decrease with time. It is noted that the topological evolution of the GLFE lattice is essentially associated with the evolution of the two types of junctions, which can be ascribed to the shrinking of small domains and the growth of large domains. The conjunctions attached to these small domains will either split or disappear upon disappearance of those small domains. If the junction density is denoted by ρ, its reciprocal $1/\rho$ is in fact equivalent to the average domain

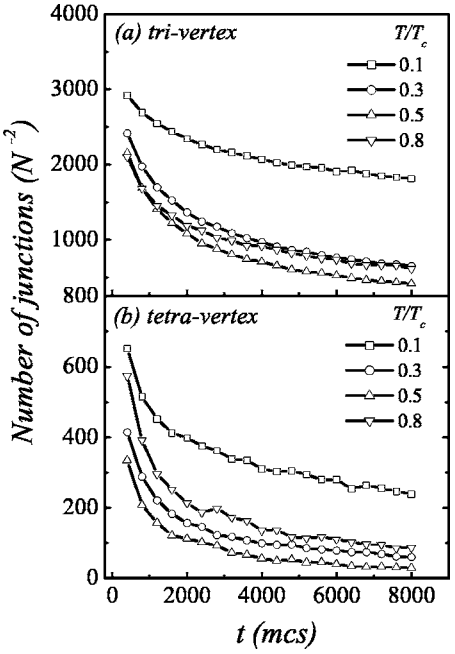

FIG. 6. Number of trijunctions and tetrajunctions as a function of time t at T/T_c=0.1, 0.3, 0.5, and 0.8. (a) for trijunctions, (b) for tetrajunctions.

area $\langle A \rangle$,[20] as shown in Fig. 7. A good linear dependence of the reciprocal density $(1/\rho)$ on time t is demonstrated.

D. One-parameter scaling

Finally, we would like to check the one-parameter scaling behavior for the asymptotic regime of the evolution, which evidences that the kinetic evolution of the domained structure can be described by a single characteristic length $l(t)$ or domain area $A(t)$. Earlier studies on domain growth adopted time-dependent structure factors to characterize the microstructure,[2,10,14] that applies to the scaling supposition perfectly. While for models including many isolated domains the domain-size distribution function[17,18] has much more direct physical connotation and is well used. Therefore, in order to make our work easier to handle, we take the average domain area $A(t)$ as the single parameter for scaling in the

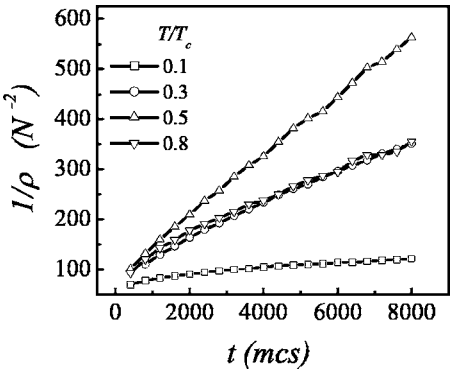

FIG. 7. Reciprocal density of junctions $(1/\rho)$ as a function of time t at T/T_c=0.1, 0.3, 0.5, and 0.8.

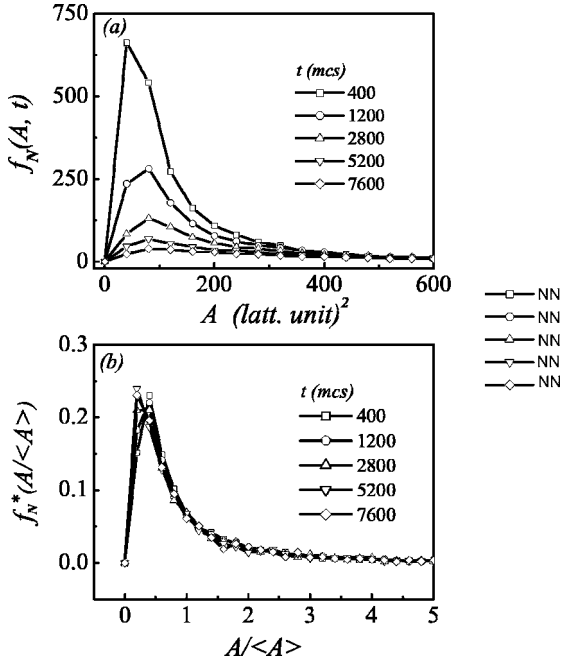

FIG. 8. (a) Domain-size distribution function $f_N(A,t)$ at different times. (b) Scaling function $f_N^*(A/\langle A(t)\rangle)$ at different times.

present work. Two types of distribution functions are adopted to characterize the domained structure. One is $f_N(A,t)$, which counts the number of domains with the area falling into span $[A, A+\Delta A]$. The other is $f_A(A,t)$, which can be explained as a probability for arbitrary sites being located in a domain with area $A(t)$ in a given span set. The relationship between the two functions is $f_A(A,t)=Af_N(A,t)/A_{all}$, where A_{all} is the sum of areas of all domains in the system, which is an in-

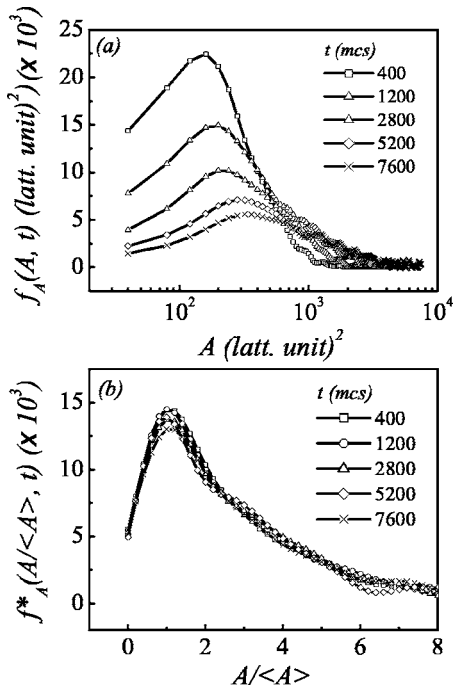

FIG. 9. (a) Domain-size distribution function $f_A(A,t)$ at different times. (b) Scaling function $f_A^*(A/\langle A(t)\rangle)$ at different times.

variant. The evaluated $f_N(A,t)$ and $f_A(A,t)$ at $T/T_c=0.3$ for $t=400$, 1200, 2800, 5200, and 7600 mcs are plotted in Figs. 8(a) and 9(a), respectively. A large number of small domains are detected in the early stage, subsequently the distribution becomes narrow and shows a single-peaked pattern with a long tail toward big $A(t)$ side. Towards the late stage, the peak shifts to the right side as the distribution becomes lower and wider due to the shrinking of small domains and the growth of larger ones. We rescale the domain size using the average domain size $\langle A(t)\rangle$ at given time t, and the rescaled data are presented in Figs. 8(b) and 9(b), respectively. The corresponding scaling functions are $f_N^*(A/\langle A(t)\rangle)$ and $f_A^*(A/\langle A(t)\rangle)$, noting that $f_N^*(A/\langle A(t)\rangle)$ is normalized by the total number of domains $N(t)$. For each type of scaling, all of the domain-size distribution data at different times fall on the same curve, demonstrating that the domain-size distribution can be described by the unique function and the kinetic evolution of the domained structure can be characterized by the unique length $\langle A(t)\rangle$ as a linear function of time t in the late stage. Hence, it can be concluded that one-parameter universal scaling behavior stands in the domain structure described by the GL ferroelectric model.

IV. CONCLUSION

In conclusion, we have investigated the kinetics of domain growth for a two-dimensional Ginzburg-Landau ferroelectric lattice with long-range Coulomb interaction, using the Monte Carlo simulation. A significant domain growth phenomenon has been observed and the power-law kinetics of domain growth has been revealed. In addition, the coexistence of trijunctions and tetrajunctions in this GLFE lattice has been verified and explained by the competition of the Coulomb interaction and gradient energy. The one-parameter scaling of the domain-size distributions at a late stage of evolution has been demonstrated. The present work has demonstrated that the domain growth in the GLFE lattice follows the kinetics for normal domain growth as well established in isotropic domain growth systems.

ACKNOWLEDGMENTS

This work was supported by the National Natural Science Foundation of China (Contract Nos. 50332020, 10021001, and 10474039) and National Key Projects for Basic Research of China (Project Nos. 2002CB613303 and 2004CB619004).

*Corresponding author. Electronic mail: liujm@nju.edu.cn

[1] A. J. Bray, Adv. Phys. **51**, 481 (2002).
[2] A. Sadiq and K. Binder, Phys. Rev. Lett. **51**, 674 (1983).
[3] Z. W. Lai, Gene F. Mazenko, and Oriol T. Valls, Phys. Rev. B **37**, 9481 (1988).
[4] Peng Wei Zhu, J. W. White, and J. E. Epperson, Phys. Rev. E **62**, 8234 (2000).
[5] Kipom Kim and Hyuk Kyu Pak, Phys. Rev. Lett. **88**, 204303 (2002).
[6] F. D. A. Aarão Reis and R. B. Stinchcombe, Phys. Rev. E **71**, 026110 (2005).
[7] Boris Levitan and Eytan Domany, Int. J. Mod. Phys. B **10**, 3765 (1996).
[8] H. V. Atkinson, Acta Metall. **36**, 469 (1988), and references therein.
[9] Gene F. Mazenko, Oriol T. Valls, and F. C. Zhang, Phys. Rev. B **31**, 4453 (1985).
[10] Man-hot Lau, Chandan Dasgupta, and Oriol T. Valls, Phys. Rev. B **38**, 9024 (1988).
[11] J.-M. Liu, Mater. Lett. **26**, 327 (1996).
[12] Subir K. Das and Sanjay Puri, Phys. Rev. E **65**, 026141 (2002).
[13] F. Corberi, A. Coniglio, and M. Zannetti, Phys. Rev. E **51**, 5469 (1995).
[14] A. Coniglio, P. Ruggiero, and M. Zannetti, Phys. Rev. E **50**, 1046 (1994).
[15] R. B. Stinchcombe, A. Misra, and B. K. Chakrabarti, Phys. Rev. E **59**, R4717 (1999).
[16] Britta Nestler, Harald Garcke, and Biom Stinner, Phys. Rev. E **71**, 041609 (2005).
[17] Long-Qing Chen and Wei Yang, Phys. Rev. B **50**, 15752 (1994).
[18] J.-M. Liu, L. C. Lim, and Z. G. Liu, Phys. Rev. B **60**, 7113 (1999).
[19] J.-R. Lee, S. J. Lee, B. Kim, and Iksoo Chang, Phys. Rev. E **54**, 3257 (1996).
[20] Attila Szolnoki and G. Szabó, Phys. Rev. E **70**, 027101 (2004).
[21] A. Kazaryan, Y. Wang, S. A. Dregia, and Bruce R. Patton, Phys. Rev. B **61**, 14275 (2000).
[22] H. Gilhój, Claus Jeppesen, and Ole G. Mouritsen, Phys. Rev. E **52**, 1465 (1995).
[23] David A. Huse and Christopher L. Henley, Phys. Rev. Lett. **54**, 2708 (1985).
[24] D. Le Floc'h, P. Bellon, and M. Athènes, Phys. Rev. B **62**, 3142 (2000).
[25] T. Miyazaki, H. Imamura, and T. Kozakai, Mater. Sci. Eng. **77**, 125 (1986); C. A. Laberge, P. Fratzl, and J. L. Lebowitz, Phys. Rev. Lett. **75**, 4448 (1995).
[26] R. Wagner and R. Kampmann, in *Materials Science and Technology: A Comprehensive Treatment*, edited by R. W. Cahn, P. Haasen, and E. J. Kramer (VCH Publishers, New York, 1991), Vol. 5, p. 213.
[27] E. N. M. Cirillo, G. Gennella, and S. Stramaglia, Phys. Rev. E **56**, 5065 (1997).
[28] H. L. Hu and L. Q. Chen, Mater. Sci. Eng., A **A238**, 182 (1997).
[29] S. Semenovskaya and A. G. Khachaturyan, J. Appl. Phys. **83**, 5125 (1998).
[30] J.-M. Liu, X. Wang, H. L. W. Chan, and C. L. Choy, Phys. Rev. B **69**, 094114 (2004).
[31] W. Cao and L. E. Cross, Phys. Rev. B **44**, 5 (1995); S. Nuambu and D. A. Sagala, *ibid.* **50**, 5838 (1994).
[32] G. Arlt, J. Mater. Sci. **25**, 2655 (1990).
[33] B. G. Potter, Jr., V. Tikare, and B. A. Tuttle, J. Appl. Phys. **87**, 4415 (2000).
[34] K. De' Bell, A. B. MacIsaac, and J. P. Whitehead, Rev. Mod. Phys. **72**, 225 (2000).